ADVANCES IN ATMOSPHERIC SCIENCES, VOL. 31, MARCH 2014, 396–406

The Characteristics of Atmospheric Ice Nuclei Measured at Different Altitudes in the Huangshan Mountains in Southeast China

JIANG Hui[1], YIN Yan*[1], YANG Lei[1], YANG Shaozhong[2], SU Hang[3], and CHEN Kui[1]

[1]*Key Laboratory for Aerosol–Cloud–Precipitation of the China Meteorological Administration, Nanjing University of Information Science and Technology, Nanjing* 210044

[2]*Chinese Academy of Meteorological Sciences, Beijing* 100081

[3]*Key Laboratory of Meteorological Disaster of the Ministry of Education, Nanjing University of Information Science and Technology, Nanjing* 210044

(Received 4 March 2013; revised 10 June 2013; accepted 17 June 2013)

ABSTRACT

The concentration of ice nuclei (IN) and the relationship with aerosol particles were measured and analyzed using three 5-L mixing cloud chambers and a static diffusion cloud chamber at three altitudes in the Huangshan Mountains in Southeast China from May to September 2011. The results showed that the mean total number concentration of IN on the highest peak of the Huangshan Mountains at an activation temperature (T_a) of -20°C was 16.6 L^{-1}. When the supersaturation with respect to water (S_w) and with respect to ice (S_i) were set to 5%, the average number concentrations of IN measured at an activation temperature of -20°C by the static diffusion cloud chamber were 0.89 and 0.105 L^{-1}, respectively.

A comparison of the concentrations of IN at three different altitudes showed that the concentration of IN at the foot of the mountains was higher than at the peak. A further calculation of the correlation between IN and the concentrations of aerosol particles of different size ranges showed that the IN concentration was well correlated with the concentration of aerosol particles in the size range of 1.2–20 μm. It was also found that the IN concentration varied with meteorological conditions, such as wind speed, with higher IN concentrations often observed on days with strong wind. An analysis of the backward trajectories of air masses showed that low IN concentrations were often related to air masses travelling along southwest pathways, while higher IN concentrations were usually related to those transported along northeast pathways.

Key words: atmospheric ice nuclei, mixing cloud chamber, static diffusion cloud chamber, deposition nucleation, condensation freezing nucleation

Citation: Jiang, H., Y. Yin, L. Yang, S. Z. Yang, H. Su, and K. Chen, 2014: The characteristics of atmospheric ice nuclei measured at different altitudes in the Huangshan Mountains in Southeast China. *Adv. Atmos. Sci.*, **31**(2), 396–406, doi: 10.1007/s00376-013-3048-5.

1. Introduction

Aerosol particles can act as cloud condensation nuclei (CCN) or ice nuclei (IN), affecting the formation and physical properties of clouds. Ice nucleation in clouds can proceed through two different pathways: homogenous and heterogeneous nucleation. Experimental tests have shown that significant homogenous nucleation usually proceeds at temperatures below -38°C and near water saturation. Meanwhile, heterogeneous ice nucleation can proceed at a relative humidity closer to ice saturation and at temperatures significantly higher than -38°C (Vali, 1991; Mathews et al., 2007). Heterogeneous ice nucleation pathways (or modes) include deposition nucleation (ice embryos forming from the vapor phase), condensation freezing (condensation followed by freezing), immersion freezing (freezing by a particle previously immersed in a water drop), and contact freezing (freezing initiated by an aerosol particle colliding with a water drop). Studies have shown that IN carry the same importance as CCN in most weather processes, and have a major impact on cloud structure and precipitation formation, as well as the radiative properties of clouds (You et al., 2002). The impact of IN on cold cloud properties is complex and is also dependent on cloud dynamics (Gierens, 2003; Haag and Kärcher, 2004; Kärcher, 2004). In addition, modern cloud seeding activities for rain-enhancement are mainly based on the hypothesis that the concentration of IN is insufficient in the natural clouds.

There are a lot of instruments and methods that can be used to measure IN. Aerosols can be sampled on filters and analyzed through exposure to water saturation conditions at different temperatures in the laboratory (Bigg, 1973). Some scholars have used a mixing cold chamber to measure IN by

* Corresponding author: YIN Yan
Email: yinyan@nuist.edu.cn

bringing ambient air into the chamber and counting the number of ice crystals that fall onto a plate of sucrose solution (Bigg and Hopwood, 1963; Bigg, 1990). Other investigators have measured concentrations of IN by counting the number of supercooled drops that freeze in a free-falling freezing tube (Saxena and Weintraub, 1988; Junge and Swanson, 2008).

Many observational studies of IN have been conducted in recent decades through field measurements and laboratory experiments. DeMott et al. (2003) observed IN near the tropopause at activation temperatures (T_a) of between -40°C and -15°C in September 2001 using a continuous flow diffusion chamber (CFDC) designed by Rogers et al. (1998). Their results showed that the concentration of IN was in the range 0.1–500 L^{-1}, depending on the temperature and humidity of the air. Santachiara et al. (2010) conducted an experiment to measure IN in different size ranges of particulate matter (PM_1, $PM_{2.5}$, PM_{10}) and total suspended particles (TSP). They found that aerosol particles in PM_1 contributed about 50% of the measured IN number concentration, but PM_{10} contributed about 70%–90%, and indicated that the dominant fractions of aerosol particles that can be activated as IN involve particles with aerodynamic diameters of less than 10 μm. Klein et al. (2010) measured the number concentration of IN at a mountain site in Central Europe during a dust transport episode in May 2008. Their results showed that IN and mineral dust were well correlated, especially with aerosol surface area, and suggested that dust might be a main constituent of ice-nucleating aerosols in that region. Ardon-Dryer et al. (2011) investigated aerosols as immersion freezing nuclei sampled at the South Pole station during January and February 2009 using a diffusion cloud chamber, the FRIDGE-TAU. Their analysis revealed that all the drops froze between -18°C and -27°C, and 50% of the drops froze at the temperature of -24°C.

Many investigators have reported that mineral dust particles could be good IN and usually nucleate at low relative humidity and rather high temperatures (Kanji and Abbatt, 2009; Kulkarni and Dobbie, 2010; Klein et al., 2010; Broadley et al., 2012). Schnell and Vali (1976), Vali et al. (1976), Levin et al. (1987) and Möhler et al. (2008) found that bio-aerosols can also be IN at a warmer temperature than mineral dust. Pratt et al. (2009) used a counterflow virtual impactor (CVI) to collect the ice particles in a cloud and found that one third of them contained biological markers. Soil particles containing black carbon are also known to act as IN, but require much higher relative humidity and lower temperatures for activation compared to mineral dust and bio-aerosols (Levin et al., 1987; DeMott et al., 1999; Dymarska et al., 2006). Aerosols of anthropogenic emissions can also affect IN concentrations directly or indirectly. There are also studies that have shown that secondary aerosol precursors, such as SO_2 and volatile organic compounds (VOCs) could inhibit ice formation on aerosol particles (Cziczo et al., 2009; Eastwood et al., 2009). Meanwhile, Stith et al. (2009), DeMott et al. (2010) and Chou et al. (2011) showed that it is easier for larger aerosol particles to be IN, especially those larger than 0.5 μm in diameter.

In order to understand the physical mechanisms of cloud and precipitation formation, and to assist with the development of techniques to possibly enhance precipitation artificially in drought regions of China, many observational studies of atmospheric IN using a variety of methods have been conducted in the country during recent decades: You et al. (1964, 2002) in Beijing; Zhao et al. (1965) in Lanzhou; Wang et al. (1965) in Baicheng; Niu et al. (2000) in the Helanshan Mountains; Li and Huang (2001) in Maqu; and Ma et al. (2002), Li et al. (2003) and Shi et al. (2006) in the Henan region of Qinghai in the northeast of the Tibetan Plateau. However, most previous studies have been conducted in northern China, with very few measurements having been taken over southern China. In the present study, field experiments were carried out on a mountain site in Anhui Province, Southeast China, to understand the background of IN in this region.

Observations were made simultaneously at three different altitudes in the Huangshan Mountains in order to analyze the characteristics of IN concentration in high-elevation areas in Southeast China and to understand how the concentration of IN varies with altitude. Two types of IN cloud chambers and aerosol instruments were simultaneously used to make the observations so as to adequately understand the characteristics of IN concentrations and their relationships with aerosol particles.

2. Methodology and instrumentation

Three observation sites were chosen at different altitudes in the Huangshan Mountains, including one located at the Guangmingding peak [(30.08°N, 118.09°E); 1840 m above sea level (a.s.l.)], one on the mountainside [(30.07°N, 118.09°E); 1351 m a.s.l.], and one near the foot of the mountains [(30.03°N, 118.09°E); 464 m a.s.l.]. The highest peak of the Huangshan Mountains is the highest point in Southeast China. Observations of IN and aerosol particles were carried out simultaneously at the three altitudes during May to September 2011. Three 5-L portable mixing cloud chambers and a static diffusion chamber were used to measure IN concentrations through different nucleation mechanisms, and a TSI 3321 Aerodynamic Particle Sizer (APS) was also used to measure the spectral distributions of aerosol particles. These instruments were operated four times daily at 0200, 0800, 1400 and 2000 LST. At the same time, aerosol particles were collected on membrane filters, which were later analyzed in the static cloud chamber. For the sampling of IN, 240 L of air was pumped at 120 L min^{-1} through a precipitator, which deposited aerosol particles on the surface of four membranes with a diameter of 47 mm and pore size of 0.45 μm. These samples were subsequently analyzed at specified temperature and supersaturation in the static diffusion chamber for their IN numbers. Aerosols were sampled on membranes eight times a day over the period 0200–2300 LST. Four membranes were sampled simultaneously. The mean flow rate was 120 L min^{-1} with a sampling time of 2 min. The volume of ambient air for each membrane was 60 L. A brief introduc-

tion to the instruments is given below.

2.1. *The 5-L portable mixing cloud chamber*

The total concentration of IN of all nucleation modes was measured by the 5-L portable mixing cloud chamber (Yang et al., 2007). At the bottom of the cloud chamber is a sugar plate lift. At the beginning of an experiment, the sugar plate is placed at the top of the cloud chamber. When the internal temperature of the chamber has cooled to the desired temperature, the sugar plate is lowered to the bottom of the chamber and the chamber is then filled with 5 L of air. Then, water steam produced by an ultrasonic fog generator is pumped into the chamber, so the IN in the air within the chamber form ice crystals. When the ice crystals grow to a certain size, they fall down to the sugar solution. The sugar plate is then raised, allowing the number of IN to be read. In this way, the cloud chamber can simulate all aerosol nucleation mechanisms.

2.2. *The static diffusion chamber*

The static diffusion chamber was used to measure IN concentrations active as deposition and condensation freezing nuclei (Yang et al., 1995). The chamber consists of two flat parallel chrome-plated brass plates of $140 \times 140 \times 5\,\mathrm{mm}^3$ each, which can be cooled independently. The internal height of the cloud chamber is 8 mm. The upper plate acts as the ice surface and is the water vapor source for ice activation and growth. The lower plate is designed to support and cool the sampled membranes, which were soaked in petroleum jelly to enhance their thermal contact with the lower plate; thus, the temperature of the lower plate is the same as that of the membrane. The temperature of the ice surface on the upper plate was higher than the lower plate. Water vapor diffuses from the upper plate to the lower one. By changing the temperature difference between the upper and lower plates, IN activated under different temperature and humidity can be measured. Deposition nuclei can form ice crystals when the moisture content is supersaturated with respect to ice, while aerosol particles that have hygroscopic ingredients can also act as condensation freezing nuclei and produce ice crystals when the moisture in the air reaches supersaturation with respect to water. The supersaturation ratio in the chamber is determined by the temperature of the upper and lower plates. The main advantage of the static diffusion chamber is that the temperature can be controlled precisely within an accuracy of 0.01°C.

The supersaturation in the chamber is calculated based on the temperature of the upper and lower plates. If the temperature of the upper and lower plates is T_1 and T_2, respectively, the supersaturation with respect to water (S_w) and with respect to ice (S_i) is determined by the temperature difference of the upper and lower plates $(T_1 - T_2)$ [see Eqs. (1) and (2)], if there is no sink for water vapor.

$$S_\mathrm{i} = \frac{E_\mathrm{i}(T_1) - E_\mathrm{i}(T_2)}{E_\mathrm{i}(T_2)} \times 100\%\,, \tag{1}$$

$$S_\mathrm{w} = \frac{E_\mathrm{i}(T_1) - E_\mathrm{w}(T_2)}{E_\mathrm{w}(T_2)} \times 100\%\,. \tag{2}$$

Here, $E_\mathrm{i}(T)$ is the supersaturated vapor pressure with respect to ice when the temperature is T, and $E_\mathrm{w}(T)$ is the supersaturated vapor pressure with respect to water when the temperature is T.

Santachiara et al. (2010) indicated that the actual relative humidity and supersaturation over the filter surface are always lower than the theoretically calculated values, owing to vapor depletion by hygroscopic particles or mixed particles and by growing ice crystals. This could be the case especially when the moisture content is low. However, if the moisture content in the chamber is sufficiently high, as for the conditions considered here (see section 3), the influence of hygroscopic particles and growing ice crystals should be negligible.

Based on Eqs. (1) and (2), the supersaturation (S_w or S_i) can be calculated based on T_1 and T_2. Similarly, in the case of known T_2 and the supersaturation (S_w or S_i), the temperature of the upper plate (T_1), which needs to be set on the instrument, can also be calculated. For example, when the temperature of the lower plate (T_2) is set to -20°C and has a maximal fluctuation of 0.05°C, and S_w is 5%, the temperature of the upper plate (T_1) will be -17.9°C to -17.8°C. Then, using these values of T_1 and T_2, the actual S_w can be obtained as 3.79%–5.68%. So, the fluctuation error of the supersaturation is less than 1.5%. For other conditions of temperature and saturation, it can also be shown that the fluctuation error of supersaturation is less than 1.5%. This is much less than the uncertainty of the instrument reported by Santachiara et al. (2010), indicating that the static diffusion chamber used in this study is reliable.

2.3. *Other instruments and the model*

Several studies (e.g., Stith et al., 2009; DeMott et al., 2010; Chou et al., 2011) have shown that larger aerosol particles are more efficient IN, especially for particles greater than 0.5 μm in diameter. In order to explore the relationship between concentrations of IN and aerosol particles, aerosol size spectra were also measured simultaneously by a TSI 3321 APS for particles in the range of 0.5–20 μm in diameter. The time resolution of the APS was 1 second.

To understand how IN concentration varies with air masses of different origin, we also used the National Oceanic and Atmospheric Administration (NOAA) Hybrid Single-Particle Lagrangian Integrated Trajectory (HYSPLIT) model (Draxler and Hess, 1998) to simulate the sources of air masses that influenced the sampling sites. We then used the results to separate the types of 36-h back trajectories of the air masses during the IN sampling period at the top of the Huangshan Mountains to study the effects of long-range transport and local air masses on IN sampled at the experimental sites.

In this study, the ambient aerosol particles were also collected by a multi-level series percussive classified aerosol sampler (NanoMoudi-II$^{\mathrm{TM}}$125A). This sampler is a 13-stage cascade impactor and the flow rate is 10 L min^{-1}. The cut-off size diameter ranges from 0.01 μm at the first stage to 18 μm at the last stage. Ranges of available cut-off size diameters are 0.01–0.018 μm, 0.018–0.032 μm, 0.032–0.056 μm,

0.056–0.1 μm, 0.1–0.18 μm, 0.18–0.32 μm, 0.32–0.56 μm, 0.56–1.0 μm, 1.0–1.8 μm, 1.8–3.2 μm, 3.2–5.6 μm, 5.6–10 μm, and 10–18μm. The filter used in NanoMoudi is a 47-mm diameter Teflon filter for collecting aerosols. The sampling time was 1 h. After sampling, the filters were analyzed in the static diffusion chamber for IN counting.

3. Results and discussion

3.1. *Seasonal variation in IN at the peak of the Huangshan Mountains*

Ice nuclei comprise a type of aerosol particle in the atmosphere that has different physical and chemical properties in different seasons. Table 1 shows the characteristics of IN concentrations under an activation temperature of −20°C in different seasons at the peak of the Huangshan Mountains. At $T_a = -20$°C, the average value of the total IN concentration measured by the mixing cloud chamber was 16.6 L^{-1}, and the IN concentrations with 5% of supersaturation with respect to water (S_w) and with respect to ice (S_i) measured by the static diffusion chamber were 0.890 L^{-1} and 0.105 L^{-1}, respectively. The observation results of these two chambers varied greatly, and the reasons for the large differences between these data were as follows. Firstly, the saturation ratios in the two chambers differed greatly. The mixing chamber provided sufficient water vapor and water droplets so that almost all the IN could be activated, while the supersaturation was set to 5% for S_w and S_i in the static diffusion chamber. Secondly, the aerosol activation conditions were different in the two cloud chambers. In the mixing cloud chamber, the aerosols were activated and grew under conditions closer to those in actual clouds, while the measured aerosols in the static diffusion chamber were formed on aerosol particles sampled on filters. Thirdly, the measurement errors and the accuracy of the two cloud chambers were not the same, which could also have led to the differences in IN concentrations.

During the observation period, with the water vapor conditions varying from $S_i = 5\%$ to $S_w = 5\%$, the mean concentration of IN increased from 0.195 to 1.282 L^{-1} in the spring, from 0.038 to 0.636 L^{-1} in the summer, and from 0.082 to 0.753 L^{-1} in the autumn. This means that higher supersaturation leads to more aerosol particles being activated, and the concentrations of IN are the highest in the spring, followed by autumn, and the lowest is in the summer. This is possibly due to a greater abundance of soil dust particles in spring and autumn, while in summer more frequent rainfall could wash out a large number of IN.

Table 2 shows a comparison of IN concentrations obtained in this study and some results reported in previous studies at different locations via mixing cloud chambers at the same activation temperature. It can be seen that the concentration of IN in the Huangshan Mountains is higher than both Baicheng, northeast China, and Beijing in the 1960s, but is lower than Beijing in the 1990s. You et al. (2002) showed that the concentration of IN increased approximately 15-fold in nearly 30 years in Beijing, and attributed the trend to the increase in aerosol pollution in the region. The concentration of IN in the Huangshan Mountains is also lower than that recorded in urban regions such as Nanjing. This is because, since the sampling site in the present study was located in a rural mountainous region, the levels of atmospheric aerosols and anthropogenic emissions were relatively small compared to urban areas.

Table 1. Statistical values for atmospheric IN concentration in different seasons (units for IN concentration: L^{-1}).

Nucleation mechanism	Statistical value	Spring	Summer	Autumn	Average
Concentration of total IN ($T_a = -20$°C)	average	22.764	11.346	15.724	16.611
Concentration of IN ($T_a = -20$°C, $S_w = 5\%$)	average	1.282	0.636	0.753	0.890
	maximum	1.667	1.45	1.642	–
	minimum	0.942	0.142	0.192	–
IN ($S_w = 5\%$)/IN (total)	percentage	5.63%	5.60%	4.78%	5.36%
Concentration of IN ($T_a = -20$°C, $S_i = 5\%$)	average	0.195	0.038	0.082	0.105
	maximum	0.833	0.1	0.242	–
	minimum	0.008	0.017	0.042	–
IN ($S_i = 5\%$)/IN (total)	percentage	0.86%	0.33%	0.52%	0.63%

Table 2. A comparison of IN concentrations obtained in the present study with those reported in previous studies using mixing cloud chambers (activation temperature of −20°C).

Observation site	Observation time	Volume of chamber (L)	Average concentration of IN (L^{-1})	Reference
Baicheng in Jilin	Apr–May 1964	2	5.8	Wang et al. (1965)
Beijing	Mar–Apr 1963	3.34	4.8	You and Shi (1964)
Beijing	Mar–Apr 1995	3.34	78.9	You et al. (2002)
Henan County in Qinghai	Aug 2001	3.05	31.3	Li et al. (2003)
Henan County in Qinghai	Oct 2003	3.05	47.4	Shi et al. (2006)
Nanjing	May–Sep 2011	5.0	20.112	Yang et al. (2012)
Huangshan Mountains	May–Sep 2011	5.0	16.6	Present paper

3.2. *The relationship between IN concentration and activation temperature*

The relationship between IN concentration and T_a has been studied by many investigators during the recent decades (Meyers et al., 1992; DeMott et al., 2003; Ardon-Dryer et al., 2011). It is widely recognized that the concentration of IN increases exponentially with a decrease in temperature (Pruppacher et al., 1998), which is also the basis of the parametric formula of IN used in many numerical models.

Figure 1a shows the relationship between IN concentration and T_a at $S_w = 5\%$, and $S_i = 5\%$. We can see that the concentration of IN increased exponentially with a decrease in T_a. Furthermore, under the same T_a, the concentration of IN was higher under the condition of $S_w = 5\%$ than when $S_i = 5\%$, indicating that water vapor conditions affect the ice nucleation ability of aerosols.

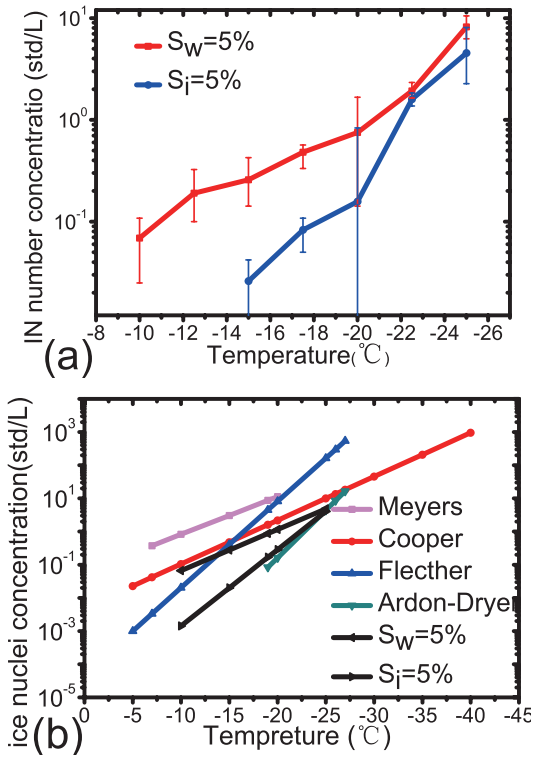

Fig. 1. (a) The relationship between IN and temperature under different water vapor conditions, and (b) a comparison with other previous results.

Fletcher et al. (1962) used the following formula to approximate the dependence of IN concentration on temperature, also referred to as the supercooling spectrum of the IN concentration:

$$N = A \times e^{-bT_a}, \tag{3}$$

where T_a is the supercooling temperature, N is the number of activated IN per unit volume of air when the supercooling temperature is T_a, and A and b are empirical parameters.

Through field observations and laboratory tests, different investigators have obtained several empirical formulae of the temperature spectrum of IN under different conditions. A comparison of the results of the present study with other previous results is shown in Fig. 1b and Table 3. As can be seen from Fig. 1b, the IN concentration of $\sim 1\ \mathrm{L}^{-1}$ at $S_w = 5\%$ and $S_i = 5\%$ was found at -19°C and -22°C, respectively, which was a little higher than that reported by Ardon-Dryer et al. (2011) obtained at a higher latitude ($\sim 1\ \mathrm{L}^{-1}$ at -23°C).

Furthermore, the concentrations of IN at $S_w = 5\%$ and $S_i = 5\%$ were very close to the results of Cooper (1980) and Ardon-Dryer et al. (2011), respectively, but were slightly lower than those reported by Meyers et al. (1992). The values obtained here at $S_w = 5\%$ were also slightly lower than those provided by Fletcher et al. (1962) for temperature lower than about -15°C, but the opposite was true for higher temperatures.

3.3. *The concentration of IN at different altitudes in the Huangshan Mountains*

Figure 2 compares the concentrations of IN at three different altitudes in the Huangshan Mountains. From Fig. 2 we can see that, as the height increased, the concentration of IN decreased, which was consistent with the concentrations of aerosol particles. As the height increases, the atmosphere becomes cleaner, so the concentration of IN will be lower. Many laboratory studies, such as Isono et al. (1959), Roberts and Hallett (1968), Zuberi et al. (2002), DeMott (2002), Archuleta et al. (2005), Knopf and Koop (2006), Marcolli et al. (2007), Eastwood et al. (2008), Kanji and Abbatt (2009), Welti et al. (2009), and Chou et al. (2011) have shown that mineral dust particles are good IN and can be activated at rather low relative humidity and high temperatures. Ardon-Dryer et al. (2011) also proved that IN concentration at the surface is higher than that at high altitude, indicating the surface could be the most important source of IN.

Table 3. Comparison of different parameterization equations of IN (units for temperature and IN concentration are $^\circ$C and L^{-1}, respectively).

	Parameterization equation	Activation temperature	Nucleation mechanism	Reference
Meyers	$N = 0.06 \times e^{-0.262 \times T}$	$T < -20^\circ$C	contact freezing	Meyers et al. (1992)
Cooper	$N = 0.005 \times e^{-0.304 \times T}$	-40°C–0°C	deposition, condensation freezing	Cooper (1980)
Fletcher	$N = 10^{-5} \times e^{-0.6 \times T}$	-27°C–0°C	deposition, condensation freezing	Fletcher (1962)
Ardon-Dryer	$N = 3 \times 10^{-7} \times e^{-0.66 \times T}$	-26°C to -19°C	immersion freezing	Ardon-Dryer et al. (2011)
Huangshan Mountains	$N = 0.0038 \times e^{-0.286 \times T}$	-10°C to -25°C	deposition, condensation freezing	Present paper
	$N = 7 \times 10^{-6} \times e^{-0.531 \times T}$		deposition	

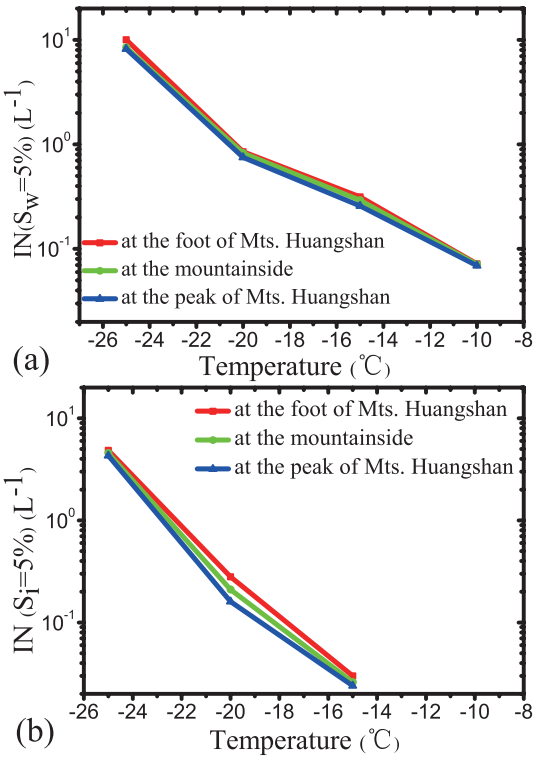

Fig. 2. The IN concentration as a function of temperature at different altitudes in the Huangshan Mountains and under different supersaturations: (a) $S_w = 5\%$; (b) $S_i = 5\%$.

3.4. *The relationship between IN concentration and atmospheric aerosols*

Previous studies (e.g., Stith et al., 2009; DeMott et al., 2010; Chou et al., 2011) have shown that larger aerosols are more efficient IN. In the present study, concentrations of IN and aerosol particles were observed simultaneously. The aerosol spectrum in the range of 0.5–20 μm was observed by the APS. For analysis, the aerosol particles were divided into two categories according to their sizes: fine particles with sizes in the range of 0.5–1.2 μm and coarse particles with sizes in the range of 1.2–20 μm. The correlation between aerosol particle number concentrations in different size segments and the IN concentration ($T_a = -20°C$, $S_w = 5\%$) was analyzed. Figures 3a–c show the correlations between IN concentration and total concentration of aerosol particles with diameters in the range 0.5–20 μm, fine particles (0.5–1.2 μm), and coarse particles (1.2–20 μm), respectively. It can be seen that the correlation was low between IN and the total concentration of aerosol particles (Fig. 3a), as well as with fine mode particles (Fig. 3b), while coarse particles (1.2–20 μm) showed a better correlation with IN number concentration (Fig. 3c), indicating that coarse particles (1.2–20 μm) make greater contributions to IN. This result was in good agreement with the results of Klein et al. (2010), who reported that IN have good correlation with aerosol particles with sizes in the range of 1.2–12 μm. These findings also confirm that it is easier for larger particles to act as IN, as proposed by DeMott et al. (2003) and Stith et al. (2009).

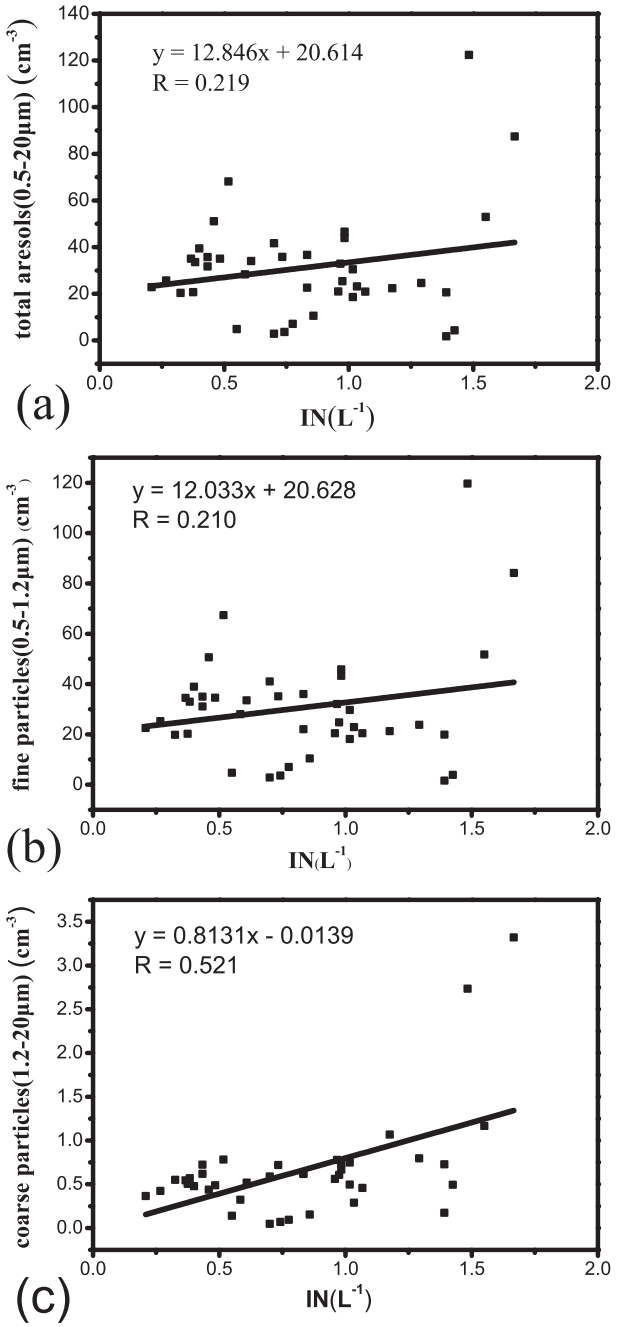

Fig. 3. The relations between IN ($T_a = -20°C$, $S_w = 5\%$) and aerosols in different size ranges: (a) 0.5–20 μm; (b) 0.5–1.2 μm; (c) 1.2–20 μm. The points are measured values and the line is a fit to those values.

The IN number concentration was significantly correlated with particle surface area, especially that of coarse mode particles. Table 4 gives the Pearson correlation coefficients of IN and the surface area of aerosol particles. As can be seen, the correlation between IN and aerosol surface area was higher than that with aerosol number concentration. This is because the ice nucleation process usually takes place on the aerosol surface. Therefore, the ice nucleation efficiency of aerosol particles should be more relevant to their surface areas, in-

Table 4. Pearson correlation coefficients between IN concentration and the number/surface area concentration of aerosol particles.

Aerosols particle size range	0.5–20 μm	0.5–1.2 μm	1.2–20 μm
Pearson correlation coefficient between IN and aerosol number concentration	0.219	0.210	0.521
Pearson correlation coefficient between IN and aerosol surface area concentration	0.317	0.234	0.539

stead of their number concentrations.

In order to understand the ice formation activity of aerosol particles of different size ranges, we conducted complementary observations in the Huangshan Mountains in September 2012. A multi-level series percussive classified aerosol sampler (NanoMoudi-II^{TM}125A) was used to collect aerosol particles of different sizes on filters, which were then later analyzed in the static cloud chamber. A total of six groups (78 copies) of observation data of IN and aerosols in different size ranges was obtained. Figures 4a–c show the size distributions of IN and aerosols, and the ratio between IN concentration and the concentration of aerosol particles (IN/aerosols) in different size ranges. The size distributions of aerosol particles were measured by a wide-range particle spectrometer (WPS) (Fig. 4b). It was assumed that the aerosol concentration measured by the WPS was equal to that collected in the filter of the NanoMoudi. So, the IN/aerosols values could be calculated and the results are shown in Fig. 4c. From Fig. 4, one can see that the concentration of IN was high in the range of 1–10 μm, and the ratio increased as the particle diameter increased, indicating that large aerosol particles are more easily activated.

3.5. *The effect of local meteorological conditions on IN*

Many investigators have reported that local meteorological conditions can affect the effectiveness of IN (Hogan, 1979; Niu et al., 2000; Ardon-Dryer et al., 2011). One local meteorological condition that could have an effect on IN concentration is wind speed. Table 5 shows the concentrations of IN and aerosol particles, and the local meteorological parameters in a period of continuous observation from 1 July to 14 July 2011 on the highest peak of the Huangshan Mountains. Each sample was collected under different wind speeds. As can be seen from Fig. 5, both the concentration of IN and aerosol particles were highly correlated with wind speed. From Table 5, one can see that high IN concentrations were often observed on days with strong wind. For example, from 1 July to 8 July, under higher wind speed (average of 7.45 m s^{-1}), the average concentration of IN was 0.851 L^{-1}. From 9 July to 14 July the average wind speed was 3.74 m s^{-1}, and the average concentration of IN was 0.395 L^{-1}. As proposed by Hogan (1979), strong winds can increase the mixing of air near the surface and lead to higher concentrations of large particles, and thus higher concentrations of IN, at higher elevations.

3.6. *The relationship between air mass trajectories and ice nuclei concentration*

In addition to local meteorological conditions, the sources of air masses also have an effect on the effectiveness of IN.

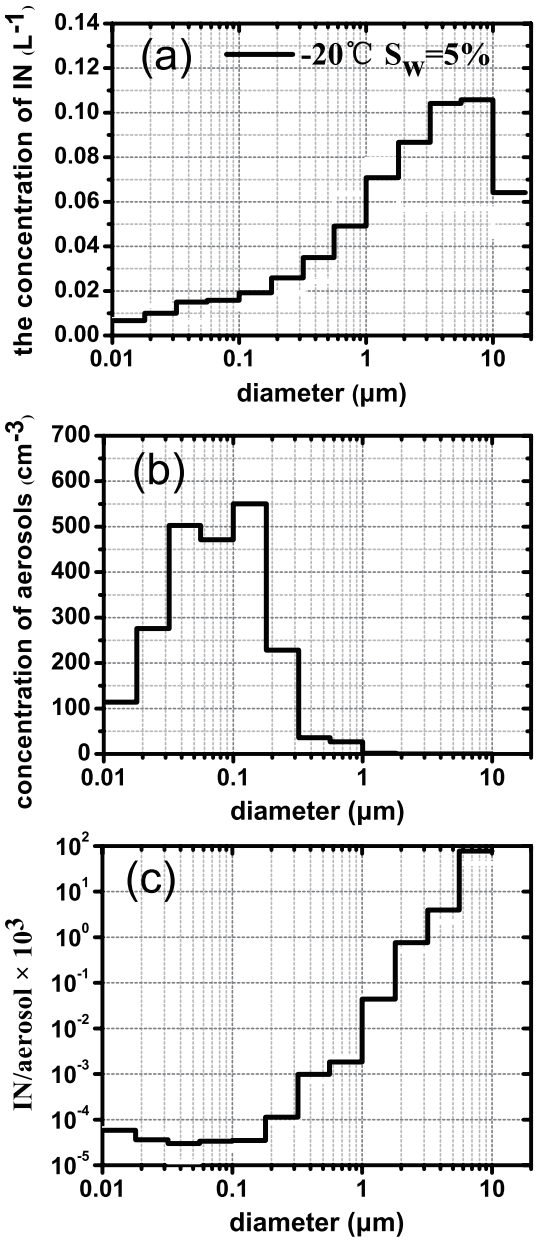

Fig. 4. The size distribution of the number concentration of (a) IN and (b) aerosols; and (c) the ratio of IN concentration in aerosol concentration (IN/aerosols) in different size ranges.

In order to understand the impact of different sources of air masses on IN concentration, the HYSPLIT model was used to separate the types of 36-h back trajectories of the air masses during the observation period on the highest peak of the Huangshan Mountains. Figure 6a shows how the air masses were divided into three types based on their incoming

Table 5. Average meteorological conditions during sampling.

Data	IN (L^{-1})	Atmospheric temperature (°C)	RH in the air (%)	Wind direction (°)	Wind speed (m s^{-1})	0.5–20 μm aerosol concentration (cm^{-3})	1.2–20 μm aerosol concentration (cm^{-3})
1 Jul 2011	1.269	17.0	95.9	229	8.50	32.35	0.66
2 Jul 2011	1.121	17.7	93.3	229	8.26	23.35	0.63
3 Jul 2011	0.942	18.2	87.7	233	9.11	33.10	0.73
4 Jul 2011	0.535	18.7	88.8	243	6.12	23.22	0.56
5 Jul 2011	0.796	18.8	90.1	241	7.95	37.65	0.60
6 Jul 2011	0.652	19.1	90.3	229	7.77	54.78	0.68
7 Jul 2011	0.821	19.2	89.4	242	6.06	33.93	0.55
8 Jul 2011	0.675	17.7	94.5	257	5.81	33.28	0.38
9 Jul 2011	0.338	18.9	90.2	99	3.16	28.21	0.39
10 Jul 2011	0.373	18.6	79.8	210	3.09	30.21	0.48
11 Jul 2011	0.569	19.0	87.0	173	3.31	26.42	0.36
12 Jul 2011	0.333	19.3	90.6	228	3.40	23.97	0.45
13 Jul 2011	0.367	20.2	90.4	251	3.84	28.77	0.53
14 Jul 2011	0.388	20.1	82.2	223	5.63	29.91	0.52

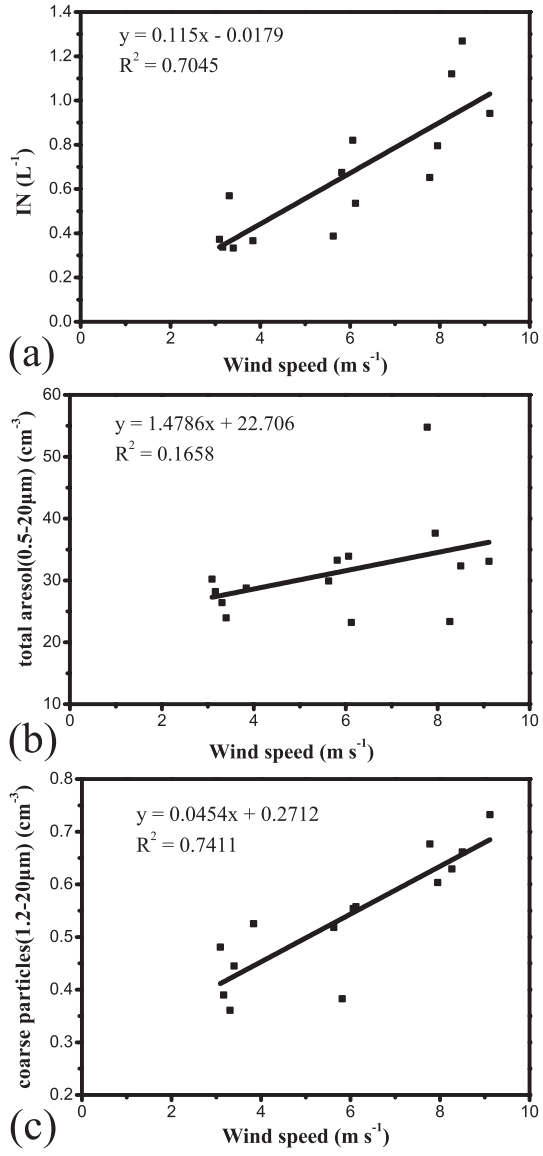

Fig. 5. The concentrations of IN ($T_a = -20°C$, $S_w = 5\%$) and aerosols as a function of wind speed. The points are measured values and the line is a fit to those values.

direction. These air masses were named as follows: local air mass (track 1); northeastern air mass (track 2); and southwestern air mass (track 3).

Figure 6b compares the IN concentrations in the three types of air mass back trajectory. As can be seen, the concentration of IN that was under the influence of the southwestern

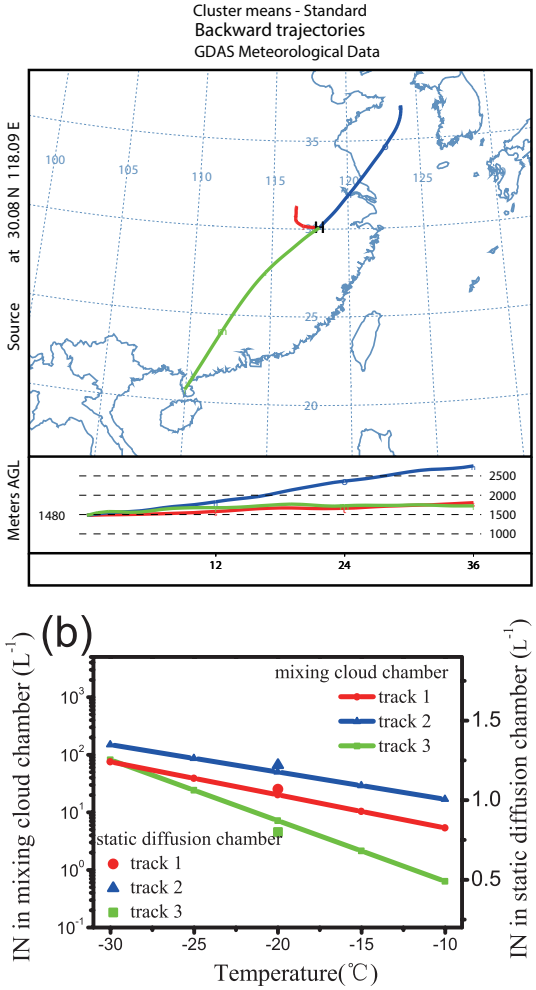

Fig. 6. (a) 36-h back trajectory analyses from the measurement site, and (b) IN concentration in different trajectories.

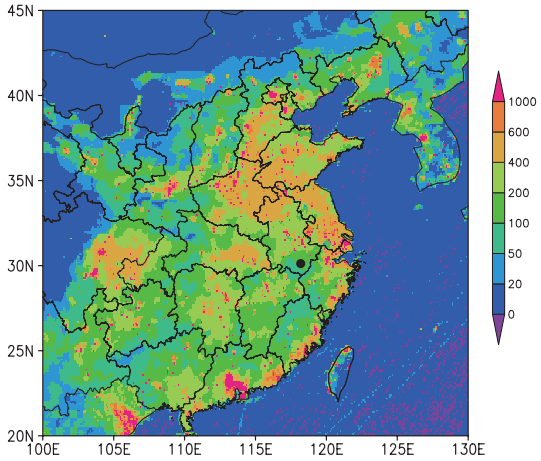

Fig. 7. The emission rate of PM_{10} [units: t yr^{-1} $(0.1\times0.1^{\circ})^{-1}$], and the black dot (30.08°N, 118.09°E) in this figure presents the position of the observation site in the Huangshan Mountains.

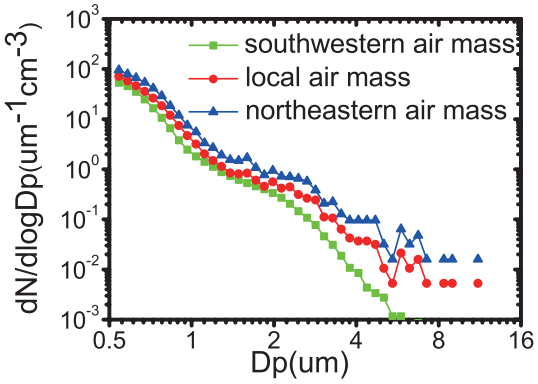

Fig. 8. The spectral distribution of aerosols in the three different air masses.

air mass was the lowest, while the highest IN concentrations were observed in the northeastern air masses. This might be due to the differences in the concentrations of aerosol particles in these three different air masses. Figures 7 and 8 show the emission rate of PM_{10} in East China, and the spectral distribution of the aerosols in the three different air masses, respectively. The emission inventory of PM_{10} was taken from EDGAR (Emission Database for Global Atmospheric Research), version 4.2. As can be seen from Fig. 7, in the northeastern direction of the measurement site are the more seriously polluted areas, and the emission rate of PM_{10} was high. Therefore, the concentration of the aerosol particles in the northeastern air mass was the highest (Fig. 8), resulting in the highest concentration of IN. On the contrary, in the observation site and its southwestern direction, the emission rate of PM_{10} was low and the air was relatively clean. Furthermore, under the influence of southwestern air masses, coarse particles were diminished in the process of long distance transport from the southeast, and the concentration of aerosol particles was low. Thus, the concentration of IN was lowest in the southwestern air mass.

Table 6 provides various statistical analyses of IN, the local meteorological conditions and atmospheric aerosols in different air masses on the highest peak of the Huangshan Mountains. During the sampling period, the ambient relative humidity in the three different air masses changed little, implying that the high IN concentration in the northeastern air mass was mainly impacted by the number concentration of aerosol particles. In addition, the ratio between the concentrations of IN and aerosol particles is given in Table 6. It can be seen that the ratio was very low, indicating that only a small fraction of the aerosol particles could act as IN, which was similar to the results reported by Bingemer et al. (2012), who studied the IN around a volcanic eruption area.

4. Conclusions

By analyzing IN data observed in the Huangshan Mountains from May to September 2011, the following conclusions can be drawn:

(1) On the highest peak of the Huangshan Mountains, when the activation temperature (T_a) was −20°C, the total number concentration of IN measured by the mixing cloud chamber was 16.6 L^{-1}. When the supersaturation was set to 5% with respect to water (S_w) and with respect to ice (S_i), the number concentrations of IN measured by the static diffusion chamber were 0.890 L^{-1} and 0.105 L^{-1}, respectively. More abundant soil dust in spring and autumn might be responsible for the higher concentrations of IN in these seasons, while in the summer more rainfall could clean a large number of IN. The concentrations of IN were very much dependent on tem-

Table 6. Statistical values of IN and aerosols in different clusters.

	Southwestern air mass	Local air mass	Northeastern air mass
Environmental relative humidity (%)	75.6	73.3	69.2
Wind speed (m s^{-1})	6.13	3.76	5.51
Concentration of IN ($T_a = -20^{\circ}C$, $S_w = 5\%$) (L^{-1})	0.8	1.068	1.217
Concentration of IN ($T_a = -20^{\circ}C$, $S_i = 5\%$) (L^{-1})	0.16	0.17	0.28
Concentration of total IN at $T_a = -20^{\circ}C$ (L^{-1})	7.2	20.15	50.30
0.5–20 μm aerosol concentration (cm^{-3})	38.47	43.38	48.98
$T_a = -20^{\circ}C$, $S_w = 5\%$, IN/total aerosol $\times10^{-5}$	2.08	2.46	2.48
$T_a = -20^{\circ}C$, $S_i = 5\%$, IN/ total aerosol $\times10^{-6}$	4.16	3.91	5.72
$T_a = -20^{\circ}C$ total IN/ total aerosol $\times10^{-4}$	1.87	4.64	10.27

perature and humidity. The concentration of IN was found to exponentially increase with a decrease in temperature, and also increased with increasing relative humidity. The concentration of IN at the foot of the mountains was higher than that at the peak, indicating that more aerosols near the ground cause high concentrations of IN.

(2) The correlation between concentrations of IN and aerosol particles of sizes in the range of 1.2–20 μm was the most significant, indicating that coarse mode aerosol particles contribute more to IN.

(3) The concentration of IN was found to vary with meteorological conditions such as wind speed, with high IN concentrations observed on days with strong wind.

(4) An analysis of the backward trajectories of air masses showed that the concentration of IN under the southwestern air mass was the lowest, and that under the northeastern air mass was the highest. This was because of the high concentration of aerosols from the northeastern direction.

Acknowledgements. This study was jointly sponsored by the National Natural Science Foundation of China (Grant No. 41030962), the Special Fund for doctorate programs in Chinese Universities (Grant No. 20113228110002), the Priority Academic Program of Development of Jiangsu Higher Education Institutions (PAPD), and the Key Laboratory for Aerosol–Cloud–Precipitation of the China Meteorological Administration (Grant No. KDW1101).

REFERENCES

Archuleta, C., P. J. DeMott, and S. M. Kreidenweis, 2005: Ice nucleation by surrogates for atmospheric mineral dust and mineral dust/sulfate particles at cirrus temperatures. *Atmos. Chem. Phys*., **5**(3), 2617–2634, doi: 10.5194/acp-5-2617-2005.

Ardon-Dryer, K., Z. Levin, and R. P. Lawson, 2011: Characteristics of immersion freezing nuclei at the South Pole station in Antarctica. *Atmos. Chem. Phys*., **11**(1), 4015–4024, doi: 10.5194/acp-11-4015-2011.

Bigg, E. K., 1973: Ice nucleus concentrations in remote areas. *J. Atmos. Sci*., **30**, 1153–1157.

Bigg, E. K., 1990: Long-term trends in ice nucleus concentrations. *Atmos. Res.*, **25**(5), 409–415.

Bigg, E. K., and S. C. Hopwood, 1963: Ice nuclei in the Antarctic. *J. Atmos. Sci.*, **20**(3), 185–188.

Bingemer, H., and Coauthors, 2012: Atmospheric ice nuclei in the Eyjafjallajökull volcanic ash plume. *Atmos. Chem. Phys.*, **12**, 12 857–12 867.

Broadley, S. L., and Coauthors, 2012: Immersion mode heterogeneous ice nucleation by an illite rich powder representative of atmospheric mineral dust. *Atmos. Chem. Phys.*, **12**(1), 287–307.

Chou, C., O. Stetzer, E. Weingartner, Z. Jurányi, Z. A. Kanji, and U. Lohmann, 2011: Ice nuclei properties within a Saharan dust event at the Jungfraujoch in the Swiss Alps. *Atmos. Chem. Phys.*, **11**, 4725–4738, doi: 10.5194/acp-11-4725-2011.

Cooper, W. A., 1980: A method of detecting contact ice nuclei using filter samples. *Preprints, Eighth International Conference on Cloud Physics*, Clermont-Ferrand, France, 665–668.

Cziczo, D. J., K. D. Froyd, S. J. Gallavardin, O. Moehler, S. Benz, H. Saathoff, and D. M. Murphy, 2009: Deactivation of ice nuclei due to atmospherically relevant surface coatings. *Environ. Res. Lett.*, **4**(4), 044013, doi: 10.1088/1748-9326/4/4/044013.

DeMott, P., 2002: Laboratory studies of cirrus cloud processes. *Cirrus*, Chapter 5, D. K. Lynch et al., Eds., Oxford University Press Inc, 102–135.

DeMott, P. J., Y. Chen, S. M. Kreidenweis, D. C. Rogers, and D. E. Sherman, 1999: Ice formation by black carbon particles. *Geophys. Res. Lett.*, **26**(16), 2429–2432, doi: 10.1029/1999GL900580.

DeMott, P. J., and Coauthors, 2003: Measurements of the concentration and composition of nuclei for cirrus formation. *Proceedings of the National Academy of Sciences of the United States of America*, **100**(25), 14 655–14 660.

DeMott, P. J., and Coauthors, 2010: Predicting global atmospheric ice nuclei distributions and their impacts on climate. *Proceedings of the National Academy of Sciences of the United States of America*, **107**(25), 17–22.

Draxler, R. R., and G. D. Hess, 1998: An overview of the Hysplit_4 modeling system for trajectories, dispersion, and deposition. *Aust. Meteor. Mag.*, **47**, 295–308.

Dymarska, M., B. Murray, L. M. Sun, M. L. Eastwood, D. Knopf, and A. Bertram, 2006: Deposition ice nucleation on soot at temperatures relevant for the lower troposphere. *J. Geophys. Res.*, **111**(D4), doi: 10.1029/2005JD006627.

Eastwood, M. L, S. Cremel, C. Gehrke, E. Girard, and A. K. Bertram, 2008: Ice nucleation on mineral dust particles: Onset conditions, nucleation rates and contact angles. *J. Geophys. Res.*, **113**(D22), 203, doi: 10.1029/2008JD010639.

Eastwood, M. L., S. Cremel, M. Wheeler, B. J. Murray, E. Girard, and A. K. Bertram, 2009: Effects of sulfuric acid and ammonium sulfate coatings on the ice nucleation properties of kaolinite particles. *Geophys. Res. Lett.*, **36**(2), 28–39, doi: 10.1029/2008GL035997.

Fletcher, N. H., P. Souires, and E. G. Bowen, 1962: *The Physics of Rainclouds*. Cambridge University Press, 408 pp.

Gierens, K., 2003: On the transition between heterogeneous and homogeneous freezing. *Atmos. Chem. Phys.*, **3**(2), 437–446.

Haag, W., and B. Kärcher, 2004: The impact of aerosols and gravity waves on cirrus clouds at midlatitudes. *J. Geophys. Res.*, **109**(D12), D12202, doi: 10.1029/2004JD004579.

Hogan, A. W., 1979: Meteorological transport of particulate material to the South Polar Plateau. *J. Appl. Meteor.*, **18**, 741–749.

Isono, K., M. Komabayasi, and A. Ono, 1959: The nature and origin of ice nuclei in the atmosphere. *J. Meteor. Soc. Japan.* **37**, 211–233.

Junge, K., and B. D. Swanson, 2008: High-resolution ice nucleation spectra of sea-ice bacteria: implications for cloud formation and life in frozen environments. *Biogeosciences*, **5**(3), 865–873, doi: 10.5194/bg-5-865-2008.

Kanji, Z. A., and J. P. Abbatt, 2009: Ice nucleation onto arizona test dust at cirrus temperatures: Effect of temperature and aerosol size on onset relative humidity. *J. Phys. Chem. A*, **114**(2), 935–941, doi: 10.1021/jp908661m.

Kärcher, B., 2004: Cirrus clouds in the tropical tropopause layer: Role of heterogeneous ice nuclei. *Geophys. Res. Lett.*, **31**(12), doi: 10.1029/2004GL019774.

Kulkarni, G. and S. Dobbie, 2010: Ice nucleation properties of mineral dust particles: determination of onset RH_i, IN active

fraction, nucleation time-lag, and the effect of active sites on contact angles. *Atmos. Chem. Phys.*, **10**, 95–105.

Klein, H., and Coauthors, 2010: Saharan dust and ice nuclei over Central Europe. *Atmos. Chem. Phys.*, **10**, 10 211–10 221.

Knopf, D. A., and T. Koop, 2006: Heterogeneous nucleation of ice on surrogates of mineral dust. *J. Geophys. Res.*, **111**(D12), doi: 10.1029/2005JD006894.

Levin, Z., S. A. Yankofsky, D. Pardes, and N. Magal, 1987: Possible application of bacterial condensation freezing to artificial rainfall enhancement. *J. Climate Appl. Meteor.*, **26**, 1188–1197.

Li, J., and G. Huang, 2001: Analysis of observational results of content of ice nuclei in the atmosphere in the upper reaches of Huanghe River. *Meteorological Monthly*, **27**(11), 8–12. (in Chinese with English abstract)

Li, S. R., G. Huang, and Z. J. Hu, 2003: Analysis of ice nuclei in atmosphere in He'nan County in upper reaches of Huanghe River. *Journal of Applied Meteorological Science*, **14**(Suppl.), 41–48. (In Chinese with English abstract)

Ma, X. C., L. G. You, and G. H. Wang, 2002: Observation and analysis of ice nuclei in Henan County of Qinghai Province in 2002. *Meteorological Monthly*, **28**(Suppl.), 22–27. (in Chinese with English abstract)

Marcolli, C., S. Gedamke, T. Peter, and B. Zobrist, 2007: Efficiency of immersion mode ice nucleation on surrogates of mineral dust. *Nucleation and Atmospheric Aerosols:* 17*th International Conference*, C. D. O'Dowd, and P. E. Wagner, Eds., Springer, 36–40, doi: 10.1007/978-1-4020-6475-3_5.

Mathews, S. R., and Coauthors, 2007: Measurements of heterogeneous ice nuclei in the western United States in springtime and their relation to aerosol characteristics. *J. Geophys. Res.*, **112**(D2), doi: 10.1029/2006JD007500.

Meyers, M. P., P. J. DeMott, and W. R. Cotton, 1992: New primary ice-nucleation parameterizations in an explicit cloud model. *J. Appl. Meteor.*, **31**(7), 708–721.

Möhler, O., and Coauthors, 2008: Heterogeneous ice nucleation activity of bacteria: new laboratory experiments at simulated cloud conditions. *Biogeosciences*, **5**(2), 1425–1435, doi: 10.5194/bg-5–1425-2008.

Niu, S. J., X. L. An, Y. Chen, and S. H. Huang, 2000: Measurements and analysis of concentrations of atmospheric ice nuclei in the Helanshan area. *Journal of Nanjing Institute of Meteorology*, **6**(2), 294–298. (in Chinese with English abstract)

Pratt, K. A., and Coauthors, 2009: *In situ* detection of biological particles in cloud ice-crystals. *Nat. Geosci.*, **2**, 398–401.

Pruppacher, H. R., J. D. Klett, and P. K. Wang, 1998: Microphysics of clouds and precipitation. *Aerosol Science and Technology*, **28**(4), 381–382.

Roberts, P., and J. Hallett, 1968: A laboratory study of the ice nucleating properties of some mineral particulates. *Quart. J. Roy. Meteor. Soc.*, **94**(399), 25–34.

Rogers, D. C., P. J. DeMott, S. M. Kreidenweis, and Y. L. Chen, 1998: Measurements of ice nucleating aerosols during SUCCESS. *Geophys. Res. Lett.*, **25**(9), 1383–1386.

Santachiara, G., L. Di Matteo, F. Prodi, and F. Belosi, 2010: Atmospheric particles acting as Ice Forming Nuclei in different size ranges. *Atmospheric Research*, **96**(2/3), 266–272.

Saxena, V. K., and D. C. Weintraub, 1988: Ice forming nuclei concentrations at Palmer Station, Antarctica. *Atmospheric Aerosols and Nucleation. Lecture Notes in Physics*, Vol. 309, Springer, Berlin, Heidelberg, 679–682.

Schnell, R. C., and G. Vali, 1976: Biogenic ice nuclei: Part I. Terrestrial and marine sources. *J. Atmos. Sci.*, **33**(8), 1554–1564.

Shi, A. L., G. G. Zheng, and L. G. You, 2006: Observation and analysis on ice nucleus of Henan County of Qinghai Province in autumn 2003. *Journal of Applied Meteorological Science*, **17**(2), 245–249. (in Chinese with English abstract)

Stith, J. L., and Coauthors, 2009: An overview of aircraft observations from the Pacific Dust Experiment campaign. *J. Geophys. Res.*, **114**(D5), doi: 10.1029/2008JD010924.

Vali, G., Ed., 1991: The report of the experts meeting on interaction between aerosols and clouds. WCRP-59 WMO/ TD-No.423, WCRP/World Climate Research Program, 265 pp.

Vali, G., M. Christensen, R. W. Fresh, E. L. Galyan, L. R. Maki, and R. C. Schnell, 1976: Biogenic ice nuclei. Part II: Bacterial sources. *J. Atmos. Sci.*, **33**, 1565–1570.

Wang, X. L., W. Y. Zhang, and S. Q. Xiong, 1965: Ice nuclei at spring in Baicheng. *Acta Meteorologica Sinica*, **35**(3), 273–279. (in Chinese with English abstract)

Welti, A., F. Lüönd, O. Stetzer, and U. Lohmann, 2009: Influence of particle size on the ice nucleating ability of mineral dusts. *Atmos. Chem. Phys.*, **9**, 6705–6715, doi: 10.5194/acp-9-6705-2009.

Yang, L., Y. Yin, S. Z. Yang, H. Jiang, H. Xiao, Q. Chen, H. Su, and C. Chen, 2012: The measurement and analysis of atmospheric ice nuclei in Nanjing. *Chinese J. Atmos. Sci.*, **37**(3), 579–594. (in Chinese with English abstract)

Yang, S. Z., P. M. Ma, and L. G. You, 1995: A static diffusion chamber for detecting atmospheric ice nuclei by using filter technique. *Acta Meteorologica Sinica*, **53**(1), 91–100. (in Chinese with English abstract)

Yang, S. Z., X. F. Lou, G. Huang, and D. X. Feng, 2007: A 15L mixing cloud chamber for testing ice nuclei. *Journal of Applied Meteorological Science*, **18**(5), 716–721. (in Chinese with English abstract)

You, L. G., and A. Y. Shi, 1964: Measurement and analysis of ice-nucleus concentration during the period from March 18th to April 30th in 1963 in Beijing. *Acta Meteorologica Sinica*, **34**(4), 548–554. (in Chinese with English abstract)

You, L. G., S. Z. Yang, X. G. Wang, and J. X. Pi, 2002: Study of ice nuclei concentration at Beijing in spring of 1995 and 1996. *Acta Meteorologica Sinica*, **60**(1), 101–109. (in Chinese with English abstract)

Zhao, J. P., M. Zhang, Y. X. Wang, Z. H. Chen, and D. J. Lai, 1965: Measurement and analysis of ice nuclei in northern of China. *Acta Meteorologica Sinica*, **35**(4), 416–422. (in Chinese with English abstract)

Zuberi, B., A. K. Bertram, C. A. Cassa, L. T. Molina, and M. J. Molina, 2002: Heterogeneous nucleation of ice in $(NH_4)_2SO_4$-H_2O particles with mineral dust immersions. *Geophys. Res. Lett.*, **29**, doi: 10.1029/2001GL014289.